

Electromagnetic excitation of anomalous acoustic waves in metals subjected to a transverse magnetic field

I. E. Aronov, T. I. Irklienko, A. P. Korolyuk, V. L. Fal'ko, and V. I. Khizhnyi

Scientific-Research Institute of Radiophysics and Electronics, Academy of Sciences of the Ukrainian SSR, Kharkov

(Submitted 2 January 1989; resubmitted 7 March 1989)

Zh. Eksp. Teor. Fiz. **96**, 287–298 (July 1989)

Experimental and theoretical investigations were made of electromagnetic excitation of sound in a metal plate, characterized by a complex dispersion law in a magnetic field \mathbf{H} perpendicular to the surface. Experiments were carried out on tungsten at frequencies $\omega/2\pi = 400\text{--}800$ MHz in magnetic fields $H \sim 100\text{--}4000$ Oe. Acoustic vibrations of two types were excited: an acoustic normal mode traveling at the velocity of sound s_0 in the metal and an anomalous (fast) sound with a phase velocity equal to the Fermi velocity of the conduction electrons $v \gg s_0$. The interaction between these two acoustic signals led to the following effects: 1) oscillations of the output acoustic signal in the magnetic field H with a constant period governed by ballistic transport of energy of the electromagnetic wave into the metal by specific electron groups; 2) resonant changes in the amplitude of these oscillations in a field H near a diamagnetic resonance at $\omega \approx \Omega$ ($\Omega = eH/mc$); 3) an inversion of the acoustic signal lines due to a change in the frequency by an amount $\Delta f \approx s_0/2d$ (d is the plate thickness) and a periodic recovery of the line profiles with a period $2\Delta f$. This theory is in good agreement with the experimental results.

1. INTRODUCTION

Electromagnetic generation of sound in metals is due to the interaction of the conduction electrons with an electromagnetic wave and with lattice vibrations. It is usual to consider the conversion of an electromagnetic wave into sound in a skin layer.^{1–14} This excites an acoustic wave representing a normal acoustic mode traveling in the metal at the velocity of sound s_0 . We shall show that under conditions of a strong spatial dispersion ($ql \gg 1$, q is the wave vector of the acoustic wave and l is the mean free path of electrons) the characteristics of the dynamics of the conduction electrons in a magnetic field applied to a metal can result in excitation of acoustic waves traveling at a velocity equal to the Fermi velocity v of electrons. These acoustic vibrations are generated in the bulk of a metal via ballistic transport of energy by an electromagnetic wave from a skin layer by specific electron groups. In other words, electrons facilitating anomalous penetration of the electromagnetic field into the investigated metal excite sound traveling at the electron velocity. We shall call these acoustic vibrations the anomalous (fast) sound. A similar physical factor results in the transport of acoustic pulses at a velocity v ("precursors"^{15,16}) by the conduction electrons in metals. The effect was first investigated^{15,16} in a geometry such that a magnetic field \mathbf{H} was parallel to the surface of the sample and perpendicular to the wave vector of sound \mathbf{q} .

We shall report experimental and theoretical investigations of electromagnetic excitation of sound in a metal plate characterized by a complex dispersion law (actual experiments were carried out on tungsten) subjected to a magnetic field \mathbf{H} perpendicular to the surface. The same geometry was used in an earlier investigation^{11,12} of electromagnetic excitation of sound as a result of the interaction of electrons with an electromagnetic field in the skin layer, but the excitation of anomalous sound was not considered because this effect was small. A Doppler-shifted cyclotron resonance and a doppleron-phonon resonance were investigated in Refs. 11 and 12. A brief communication¹⁷ on electromagnetic excita-

tion of sound in tungsten at frequencies $\omega/2\pi = 400\text{--}800$ MHz in magnetic fields $H \sim 100\text{--}4000$ Oe revealed a complex oscillatory dependence of the amplitude U of the generated sound on H . In the range of frequencies and magnetic fields used in Ref. 17 there were significant effects of the generation of anomalous sound. The amplitude of this sound was characterized by an oscillatory dependence on the magnetic field H and when the condition

$$\omega \approx \Omega \quad (1)$$

was satisfied, a diamagnetic resonance was observed (Ω is the cyclotron frequency). These oscillations were similar to the Gantmakher-Kaner oscillations¹⁸ and to the diamagnetic resonance^{19,20} due to anomalous penetration of electromagnetic waves into a metal. Interference of anomalous sound and a normal acoustic mode of the investigated metal resulted in frequency inversion of the amplitude of the generated sound $U(H)$ when the frequency was altered by an amount $\sim s_0/d$ (d is the thickness of the metal plate) and a periodic (period $2s_0/d$) recovery of the line profile.

2. EXPERIMENT

Transformation of electromagnetic and acoustic waves was investigated in transmission geometry. An acoustic signal was generated or recorded on one side of a tungsten plate and an electromagnetic one on the other. This hybrid measurement method was described in greater detail in Ref. 12. Plane-parallel tungsten plates of thickness $d \approx 1.95\text{--}2.00$ mm were cut by spark machining from a single crystal characterized by a resistivity ratio $\rho_{300\text{K}}/\rho_{4.2\text{K}} = 4 \cdot 10^4$. The low-temperature setup was described in Ref. 21. Experiments were carried out in the $\mathbf{q} \parallel \mathbf{H} \parallel [100]$ geometry at frequencies $f = \omega/2\pi = 400\text{--}800$ MHz. The magnetic field was varied within the range 0–4 kOe and measurements were made at temperatures 4.2–1.5 K. All the measurements were carried out under conditions of continuous oscillations, so that special attention had to be paid to suppress stray leakage

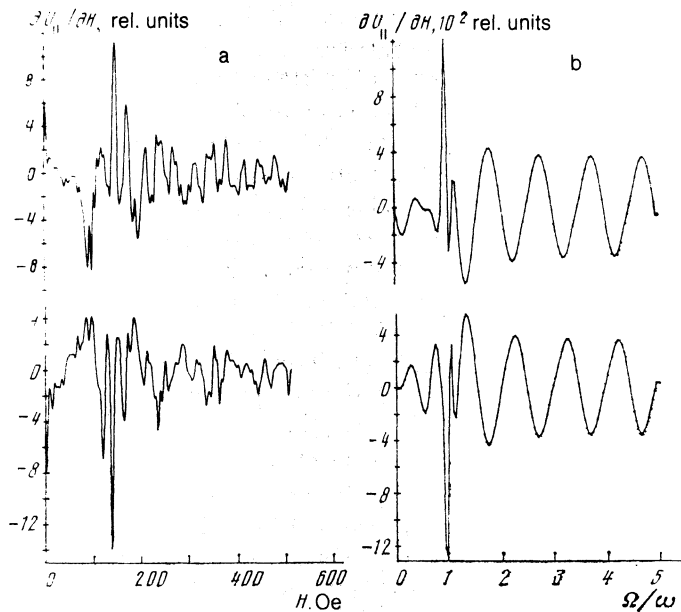


FIG. 1. Dependence of the derivative $\partial U_{\parallel} / \partial H$ on the magnetic field H : a) experimental results, the upper curve corresponds to $f = 524.09$ MHz and the lower one to $f = 523.33$ MHz; b) calculations carried out for $\omega/\nu = 10$, $d/l = 1/2$, where the upper curve corresponds to $f = 500 + \Delta f$ MHz, and the lower one to $f = 500$ MHz.

of the power to the input of the receiving channel. In all the experiments the level of such leakage was below the sensitivity threshold of the receiving channel, which was -130 – 140 dB/W. The power supplied to a sample was less than 50 mW.

Arrangements were made to record the following two components of an acoustic signal U during the same experiment: $U_{\parallel}(H) \parallel \mathbf{E}(0)$ and $U_{\perp}(H) \perp \mathbf{E}(0)$, and also the derivatives $\partial U_{\parallel} / \partial H$ and $\partial U_{\perp} / \partial H$ [$\mathbf{E}(0)$ is the intensity of the electric field on the surface of the sample $z = 0$]. The dependence of the signal $U_{\parallel}(H)$ exhibited a monotonic fall on increase in H . This dependence had been investigated by us for tungsten in an earlier study¹² at frequencies up to 150 MHz. On increase in the frequency, when its value exceeded 400 MHz, we observed oscillations in weak magnetic fields ($qR > 1$) and these oscillations modulated the monotonic $U_{\parallel}(H)$ curve (R is the Larmor radius of an electron). Figure 1a of our earlier study¹⁷ reproduced the oscillatory part of the signal $U_{\parallel}(H)$ representing a superposition of the harmonics with very different periods. These periods corresponded to different groups of carriers in tungsten. The dependence of the oscillation periods on the magnetic field was determined by a spectral analysis of the signal $U_{\parallel}(H)$ whose Fourier spectrum is shown in Fig. 1b in Ref. 17. It was established that the positions of singularities in the Fourier spectra were independent of the frequency f and that the $U_{\parallel}(H)$ oscillations due to each group had a constant period in a magnetic field.

A strong dependence of the profile of the $U_{\parallel}(H)$ lines on the frequency f was observed. A change in the frequency f by an amount $\Delta f \approx 0.7$ MHz resulted in line inversion. The line profile was restored periodically in a magnetic field when the frequency was altered at a period $2\Delta f$. The frequency inversion of the $U_{\parallel}(H, f)$ lines is shown in Fig. 2 of Ref. 17. For example, large-period oscillations were inverted in

the frequency interval $\Delta f = 0.763$ MHz.

Field dependences of the derivative $\partial U_{\parallel}(H) / \partial H$ were investigated in order to reveal resonance singularities in the signal. Figure 1a shows the derivatives of the signal $U_{\parallel}(H)$ with respect to H . A singularity in a field $H \approx 160$ Oe corresponding to the condition $\Omega = \omega$ can be seen in Fig. 1a. The line profile of $\partial U_{\parallel}(H) / \partial H$, like that of $U_{\parallel}(H)$, depended strongly on the frequency f and exhibited inversion in a frequency interval Δf . It was found that an increase in the frequency shifted the resonance in a magnetic field (in the direction of higher values of H) by an amount proportional to the frequency f .

3. THEORY

Propagation of electromagnetic and acoustic waves in a metal and their mutual transformation are described by a system of equations consisting of the Maxwell equations, a linearized transport equation for the conduction electrons, and equations describing the lattice vibrations (see, for example, Ref. 8). The boundary conditions for this system of equations are as follows: the continuity of the tangential components of the alternating electric and magnetic fields on the metal surfaces $z = 0$ and $z = d$; vanishing of the voltages on these surfaces; specular reflection of electrons from the boundary [the coordinate axes were selected as follows: $\mathbf{z} \parallel \mathbf{n}$, \mathbf{H} , \mathbf{q} ; \mathbf{n} is the normal to the surface of the metal plate; $\mathbf{x} \parallel \mathbf{E}(0)$; $\mathbf{E}(0)$ is the vector of the electric field of the electromagnetic wave in vacuum].

Outside the region of strong coupling of sound with normal electromagnetic modes in a metal, and also in the case of a weak coupling between the waves, the coefficient of conversion of an electromagnetic wave into sound is small in terms of the parameter s_0/v . In this case the equations for the electromagnetic and acoustic fields are independent in the leading approximation and the coupling of the waves occurs

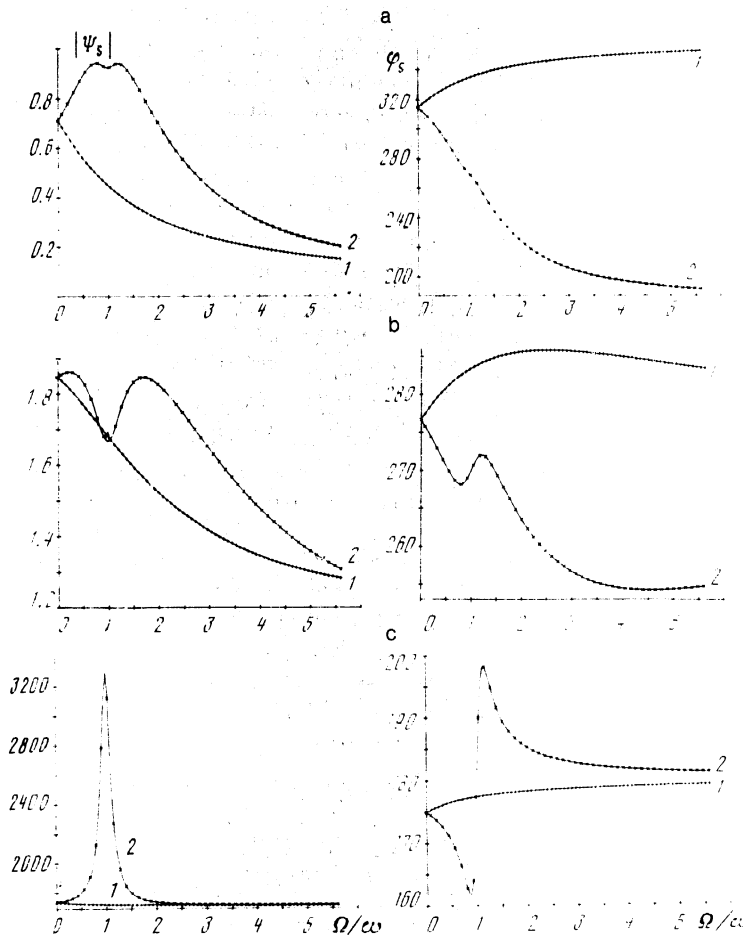


FIG. 2. Calculated dependences of $|\Psi_s|$ and φ_s on ω/Ω for $\omega/\nu = 10$: a) limiting point ($\kappa = 1$), $d/l = 1$; b) limiting section ($\omega > 1$, $\omega = 1$ or 2), $d/l = 1/2$; c) extremal drift, $d/l = 1/2$. Curves labeled 1 apply to the positive polarization and curves labeled 2 apply to the negative polarization.

in accordance with perturbation theory. When an acoustic wave propagates along a high-order symmetry axis of a crystal, the longitudinal and two transverse modes are independent. In a transverse magnetic field the equations and their solutions are simpler if we introduce circular polarization for the displacement vector \mathbf{U} : $U_s = U_x + isU_y$, where $s = \pm 1$. The acoustic wave field on the $z = d$ surface has the form¹¹ ($U_s \propto e^{-i\omega t}$)

$$U_s(d, H) = \frac{iE_s'(0)}{\pi\rho_0 s_0^2} \int_{-\infty}^{\infty} \frac{dk}{k^2 - q_s^2} \frac{k\eta_s(k)}{k^2 - 4i\pi\omega c^{-2}\sigma_s(k)} \times e^{ikd} \left[1 + \frac{iq_s}{k} \text{ctg}(q_s d) \right], \quad (2)$$

where ρ_0 is the mass density of the investigated crystal; q_s is the wave vector of sound which includes electron damping and renormalization of the velocity during propagation of sound in the metal; $\sigma_s(k)$ is a Fourier component of the electrical conductivity; $\eta_s(k)$ is a Fourier component of the "deformation conductivity"; the general form of these Fourier components can be found in Ref. 11.

Equation (2) describes electromagnetic excitation of sound by the deformation mechanism of the electron-phonon interaction. In the range of frequencies and magnetic fields of interest to us the conditions for a strong spatial inhomogeneity are realized:

$$ql \gg qR \gg 1, \quad \omega \gg \nu \quad (3)$$

(ν is the relaxation frequency of electrons). As shown in Ref. 11, in this case we can ignore the induction force in the equations describing the lattice vibrations.

It is convenient to calculate the integral in Eq. (2) along a contour in the complex k plane by closing it in the upper half-plane. The integrand has poles and branch points which are contained in the transport coefficients $\sigma_s(k)$ and $\eta_s(k)$. The branch points are due to electrons from the vicinity of a limiting point (limiting section) or of extremal drift, which effect the ballistic mechanism of anomalous penetration of an electromagnetic field into a metal.¹⁸ The positions of the poles in Eq. (2), associated with a normal acoustic wave, is given by the equation

$$k^2 = q_s^2. \quad (4)$$

Poles of the second type are of electromagnetic origin and represent the solution of the dispersion equation

$$k^2 = 4i\pi\omega c^{-2}\sigma_s(k). \quad (5)$$

In the case under discussion defined by Eq. (3) the roots of Eq. (5) correspond to the anomalous skin effect ($\text{Im } k \propto \text{Re } k$) and there are no solutions in the form of weakly damped waves characterized by $\text{Re } k \gg \text{Im } k$ (for example, doppler-sons).

It follows that the amplitude of the output sound $U_x(d)$,

H) of Eq. (2) is a sum of three terms which are damped exponentially at different distances. The first term U_{1s} , due to a pole of Eq. (4), is the amplitude of a normal acoustic wave in a metal propagating at a velocity s_0 and damped out at a depth $L_{3B} = (\text{Im } q_s^{-1}) \propto v/\omega$. The second term U_{2s} , governed by the component of the field of the anomalous skin effect, is rapidly damped out within the skin depth $\delta \approx (cp_F/3\pi^2\omega Ne^2)^{1/3} \ll L_{3B}$ (N is the concentration of quasiparticles and p_F is the Fermi momentum). The third term represents anomalous sound traveling at the velocity v in a metal. Generation of this sound is an acoustic analog of the Gantmakher-Kaner effect because it is due to the branch points of the kinetic coefficients $\sigma_s(k)$ and $\eta_s(k)$. The amplitude of this term and the electromagnetic field penetrating anomalously are damped out in a depth of the order of the mean free path of electrons l . The observed effects are associated with the interaction and competition of these three sound excitation mechanisms. At low frequencies ($\omega < \nu$) characterized by $L_{ac} \gg l$ the term U_{1s} exceeding considerably the other two terms is characterized by resonant dependences on H due to a Doppler-shifted cyclotron resonance and a doppleron-phonon resonance.^{11,12} At high frequencies when the condition (3) is satisfied and

$$l \gg L_{ac}, \quad (6)$$

the relative contribution of the term $U_{3s}(H)$ to electromagnetic excitation of sound becomes greater. In experiments on tungsten at high frequencies [defined by Eqs. (3) and (6)] the region of Doppler-shifted cyclotron resonances²²

$$\omega - q_s v_{z \text{ ext}} = r \Omega \quad (7)$$

($v_{z \text{ ext}}$ is the extremal average velocity of electrons along the vector \mathbf{H} ; r_s is an integer) and the region of doppleron-phonon resonance²³

$$\text{Re } q_s^2 = |4\pi\omega c^{-2} \text{Im } \sigma_s(q_s)| \quad (8)$$

correspond to strong magnetic fields $H > 1$ kOe. In the range $H < 1$ kOe the amplitude $U_{1s}(H)$ is a monotonic function of H and the most interesting and informative is the component U_{2s} of electromagnetic excitation of sound.

The singularities of the behavior $U_{3s}(H)$ account for the oscillatory behavior of the generation of sound by an electromagnetic field. The acoustic component U_{1s} in Eq. (2) [representing a residue of the pole of Eq. (4)] is

$$U_{1s} = -\frac{E_s'(0)}{\rho_0 \omega^2} [1 + i \text{ctg}(q_s d)] \eta_s(q_s) e^{iq_s d}. \quad (9)$$

The dependence of the deformation conductivity $\eta_s(q_s)$ on the applied magnetic field has no singularities in the range $H < 1$ kOe (Ref. 11). The phase velocity of sound described by Eq. (9) and generated in the metal is $\omega/\text{Re } q_s \approx s_0$.

The amplitude U_{3s} will be found by deriving expressions for the coefficients $\sigma_s(k)$ and $\eta_s(k)$ in Eq. (2). We shall assume that the components of the deformation potential tensor can be written in a form corresponding to an isotropic dispersion law¹³:

$$\Lambda_{sz} = \mu v_s v_z, \quad (10)$$

where μ is a coefficient with the dimensions of mass and of value which is of the same order as the cyclotron mass of the

conduction electrons. The anisotropy of the electron energy $\varepsilon = \varepsilon(\mathbf{p})$ will be allowed for in the dependence of the longitudinal velocity v_z on the phase τ of the transverse motion of electrons:

$$v_z(p_z, \tau) = \bar{v}_z(p_z) + \Delta v_z(p_z, \tau). \quad (11)$$

Here,

$$\bar{v}_z(p_z) = \frac{1}{2\pi} \oint d\tau v_z(p_z, \tau)$$

is the average velocity of electrons along \mathbf{H} .

In this model the values of $\sigma_s(k)$ and $\eta_s(k)$ for a given sheet of the Fermi surface can be expressed in terms of the same function:

$$\sigma_s(k) = \sigma_0 F_s(k),$$

$$k\eta_s = i\bar{\eta} + i\bar{\eta}_0 \frac{\omega + sr\Omega + i\nu}{\nu} F_s(k), \quad (12)$$

where

$$\sigma_0 = \frac{3iNe^2}{2m\nu}, \quad N = \frac{8\pi p_F^2}{(2\pi\hbar)^3}, \quad \bar{\eta}_0 = \frac{3}{2} Ne \left(\frac{\mu}{m} \right)$$

(σ_0 is the conductivity and N is the electron density),

$$\bar{\eta}_1 = \bar{\eta}_0 \int_{-1}^1 dt \frac{v_{\perp}^2(t)}{v} \alpha_r^*(t) a_r(t), \quad v_{\perp}^2(t) = v_x^2 + v_y^2, \quad (13)$$

$$F_s(k) = \sum_{-1}^1 \int \frac{dt [v_{\perp}^2(t)/v] \alpha_r^*(t) a_r(t) \nu}{\omega + sr\Omega + kv_z(t) + i\nu}, \quad (14)$$

$t = p_z/p$, and a_r and α_r are the Fourier coefficients:

$$\alpha_r^* = \frac{1}{2\pi} \oint d\tau e^{i\tau r} v_s(\tau, p_z) \exp \left[-\frac{ik}{\Omega} \int_0^{\tau} d\tau' \Delta v_z(\tau', p_z) \right], \quad (15)$$

$$a_r = \frac{1}{2\pi} \oint d\tau e^{-i\tau r} v_x(\tau, p_z) \exp \left[-\frac{ik}{\Omega} \int_0^{\tau} d\tau' \Delta v_z(\tau', p_z) \right].$$

The existence of a g th order symmetry of the Fermi surface (relative to rotation about the p_z axis) results in selection of the resonance serial number in the sums over r in accordance with Eq. (14) following the rule of Ref. 24:

$$r = r_s = ng + s, \quad n = 0, \pm 1, \pm 2, \dots \quad (16)$$

The function $F_s(k)$ includes branch points of the complex variable $k = k_b$, the positions of which are given by the relationship

$$\pm k_b v + \omega + rs\Omega + i\nu = 0, \quad v = v_z(p_z = p_{1,2}), \quad (17)$$

where p_1 is the momentum of electrons in the vicinity of a limiting point or section of the Fermi surface (the velocity of electrons at these points is $\mathbf{v} \parallel \mathbf{H}$), p_2 is the momentum of quasiparticles characterized by extremal drift and by

$$(\partial \bar{v}_z / \partial p_z)_{p_z = p_2} = 0. \quad (18)$$

Electrons from the vicinity of the limiting point and a limiting section give rise to a logarithmic branch point, whereas electrons characterized by an extremal drift create a root

branch point of the function $F_s(k)$ (Ref. 18).

In the case of a limiting section (limiting point), when electrons with the highest value of the momentum $p_z = p_1$ are selected, the function $F_s(k)$ is

$$F_s(k) = \frac{1}{3} \frac{\kappa^{-1/2}}{kl} \left\{ \frac{2b_s}{kl} + \left[\kappa - \left(\frac{b_s}{kl} \right)^2 \right] \ln \frac{b_s + kl}{b_s - kl} \right\}, \quad (19)$$

where $\kappa = (p_z/p_1)^2$; $p_1 \ll p$, p is the largest value of the momentum at right-angles to the vector \mathbf{H} ;

$$b_s = i + (\omega + sr\Omega)/v = i + \beta_s, \quad l = v/v.$$

In the case of an elliptic limiting point, we have $\kappa = 1$.

A section of the Fermi surface characterized by an extremal drift of carriers [Eq. (18)] gives rise to the following form of the function $F_s(k)$:

$$F_s(k) = (kl)^{-1/2} [(v_\perp/v)^2 \alpha_r^* a_r]_{p_z=p} [(kl+b_s)^{-1/2} - (kl-b_s)^{-1/2}]. \quad (20)$$

We can readily see from Eqs. (19) and (20) that the amplitude U_{1s} of Eq. (9) includes a contribution of such values of $k = q_s \gg 1/l$, for which the function $\eta_s(q_s, H)$ in Eq. (12) has no singularities. Knowing the function $F_s(k)$ [Eqs. (19) and (20)] we can readily obtain expressions for the amplitude $U_{3s}(H)$:

$$U_{3s} = U_0 \exp \left[-\frac{d}{l} + i \frac{\omega + rs\Omega}{v} d \right] \Psi_s^{(1,2)}(H, \nu), \quad (21)$$

Here,

$$U_0 = E_s'(0) \mu c^2 v / 2\pi^2 \rho_0 s_0 \omega^2 l,$$

and the functions $\Psi_s^{(1,2)}(H, \nu)$ describe the profile of a line representing electromagnetic excitation of sound. The phase

velocity of anomalous sound [Eq. (21)] is governed by the drift velocity of electrons v . The signal is analogous to an acoustic pulse generated by sound and traveling at the Fermi velocity.^{15,16} In the case of electrons corresponding to a limiting section [represented by the index (1) in Eq. (21)] we have

$$\begin{aligned} \Psi_s^{(1)}(H, \nu) &= i \int_1^\infty d\xi \left[\frac{\xi - i\beta_s}{ql} + i \right]^{-1} \left\{ \frac{f_s^{(1)}(\xi)}{\pi^2} \right. \\ &\quad \left. + \left[\kappa - \left(\frac{1 - i\beta_s}{\xi - i\beta_s} \right)^2 \right]^2 \right\}^{-1} \\ &\quad \times \exp[-d(\xi-1)/l] [\kappa - (1 - i\beta_s)^2 / (\xi - i\beta_s)^2], \\ f_s^{(1)}(\xi) &= 2 \frac{1 - i\beta_s}{\xi - i\beta_s} + \left[\kappa - \left(\frac{1 - i\beta_s}{\xi - i\beta_s} \right)^2 \right] \\ &\quad \times \left[\ln \frac{[(\xi+1)^2 + 4\beta_s^2]^{1/2}}{\xi-1} - i \operatorname{arctg} \frac{2\beta_s}{\xi+1} \right]. \quad (22) \end{aligned}$$

In the case of electrons characterized by an extremal drift [index (2) in Eq. (21)], we find that

$$\begin{aligned} \Psi_s^{(2)} &= - \int_0^\infty d\xi \left(\frac{\xi - i\beta_s}{ql} + i \right)^{-1} \left\{ \frac{\xi-1}{2} [f_s^{(2)}(\xi)]^2 - 1 \right\}^{-1} \\ &\quad \times \exp[-d(\xi-1)/l] (\xi-1)^{1/2}, \quad (23) \end{aligned}$$

$$f_s^{(2)}(\xi) = \frac{\{[(\xi+1)^2 + 4\beta_s^2]^{1/2} + (\xi+1)\}^{1/2} - i \operatorname{sgn} \beta_s \{[(\xi+1)^2 + 4\beta_s^2] - (\xi+1)\}^{1/2}}{[(\xi+1)^2 + 4\beta_s^2]^{1/2}}.$$

A calculation of the line profiles of the functions

$$\Psi_s(H) = |\Psi_s(H)| \exp[i\varphi_s(H)]$$

was carried out on a computer. Figure 2 shows the dependences of the amplitude $|\Psi_s|$ and of the phase φ_s on $x = \Omega/\omega \sim H$ in the cases of a limiting point, $\kappa = 1$ (Fig. 2a), a limiting section, $\kappa > 1$ (Fig. 2b), and extremal drift (Fig. 2c). In all cases the curves with the positive polarization are identified by the number 1, whereas those with the negative polarization are characterized by 2.

1. Limiting point ($\kappa = 1$)

In the $s = \pm 1$ polarization the functions $|\Psi_+(x)|$ and $\varphi_+(x)$ behave similarly for different values of d/l and ω/v . The dependences are monotonic and do not include a diamagnetic resonance: an increase in the field reduces $|\Psi_+(x)|$ monotonically, whereas $\varphi_+(x)$ rises monotonically and both approach constant values (curves denoted by 1).

Line profiles representing the amplitude $|\Psi_-(x)|$ and

the phase $\varphi_-(x)$ of the resonant polarization are shown in Fig. 2a (curves labeled 2). The dependence $\varphi_-(x)$ for all the values of the parameters d/l and ω/v is a monotonically decreasing function of x and has a constant value in high magnetic fields. The slope of $\varphi_s(x)$ increases on reduction in the parameters d/l and ν/ω . The graph of $|\Psi_-(x)|$ demonstrates resonant behavior due to a diamagnetic resonance. At the center of the $x = 1$ line ($\omega = \Omega$) there is a minimum of depth which increases on reduction in d/l and ν/ω . The resonance lines become narrower on reduction in the collision frequency ν .

2. Limiting section ($\kappa > 1$)

Figure 2b shows the amplitude $|\Psi_s(x)|$ and the phase $\varphi_s(x)$ for the following set of parameters: $\kappa = 1$ or 2; $\omega/v = 10$; $d/l = 1/2$. The behavior of the nonresonant functions $|\Psi_+(x)|$ and $\varphi_+(x)$ is similar to that observed in the case when $\kappa = 1$. In the presence of a limiting section a resonant singularity of the amplitude $|\Psi_-(x)|$ is manifested more strongly than at a limiting point. The relative depth of

a minimum depends on the parameters d/l and v/ω , exactly as in the preceding case.

The physical reason for the appearance of a minimum of the functions $|\Psi_-(H)|$ at a diamagnetic resonance is discrimination of electrons in the vicinity of a limiting point (limiting section) $p_z = p_1$ relative to the characteristics of their longitudinal and transverse motion. The point is that at the limiting point itself the electrons "pass through" ($\mathbf{v} \parallel \mathbf{H}$) and have no transverse motion ($v_\perp = 0$) so that their interaction with a wave of frequency ω is nonresonant. A resonance can be exhibited by electrons in the vicinity of a limiting point; these electrons are characterized by the momentum component $p_z \approx p_1 - \delta p_z$ and the velocity component $v_\perp \neq 0$ ($\delta p_z \sim 1/kl$) and they move in phase with the wave in question. Obviously, the number of the electrons passing through increases on increase in κ and also on increase in the mean free path l . Therefore, the relative depth of a minimum of the function $|\Psi_-(x)|$ at $x = 1$ increases on increase in the parameters κ and l .

3. Extremal drift

The profile of nonresonant polarization lines $|\Psi_+(x)|$ and $\varphi_+(x)$ is similar to that in the case of a limiting point. In the resonant polarization case a typical resonance pattern is observed (Fig. 2c): the function $|\Psi_-(x)|$ has a sharp maximum and its width is governed by the ratio ω/v , whereas the amplitude is determined by the parameters d/l and ω/v . The function $\varphi_-(x)$ is in the form of a dispersion curve. Naturally, in the extremal drift case of Eq. (18) the function $|\Psi_-(x)|$ has no minimum, because all the electrons belonging to this group have fixed values of the transverse velocity v_\perp ($p_z = p_2$) and at resonance ($\omega = \Omega$) they move in phase with the wave.

The intensity of a diamagnetic resonance due to the electrons described by Eq. (18) is much greater than in the case of a limiting point or a limiting section. This is due to a singularity of the density of states of the resonant electrons²⁵ and the nature of singularities of Eqs. (22) and (23).

In the range of magnetic fields far from a diamagnetic resonance ($\Omega \ll \omega$ or $\Omega \gg \omega$) the amplitudes $\Psi_s(H)$ are monotonic functions of H and are identical for both polarizations. In this range of fields H the signal $U_{3s}(H)$ representing the electromagnetic excitation of sound [Eq. (21)] is described by a harmonic function of H , which is similar to the Gantmakher-Kaner oscillations. Near a resonance ($|\omega - \Omega| < v$) the $U_{3+}(H)$ signal exhibits oscillations whereas the $U_{3-}(H)$ signal undergoes a diamagnetic resonance.

We can readily see that both the diamagnetic resonance and the oscillations are present for both components of the signal due to electromagnetic excitation of sound investigated in our experiments:

$$\begin{aligned} U_{\parallel}(H) &\equiv U_x(H) = (U_+ + U_-)/2, \quad U_{\perp}(H) \\ &\equiv U_y(H) = (U_+ - U_-)/2i. \end{aligned}$$

However, the observed dependences $|U_x(H)|$ and $|U_y(H)|$ may appear different. This is due to the following circumstance. In the investigated range of magnetic fields and frequencies [Eq. (3)] we find, to within small terms of the order of $1/ql$, that the relationships $q_+(H) \approx q_-(H)$ (see, for example, Ref. 26) and $\eta_+ \approx \eta_-$ are satisfied and that

both polarizations in the acoustic component (9) are identical: $U_{1+}(H, \omega) \approx U_{1-}(H, \omega)$ and the corresponding signal is linearly polarized along the x axis. Therefore, the projection of $U_x(H)$ represents interference between acoustic excitations of two types, whereas $U_y(H)$ is simply governed by the component of U_{3s} :

$$U_x = U_{1+} + (U_{3+} + U_{3-})/2, \quad U_y = (U_{3+} - U_{3-})/2i. \quad (24)$$

4. DISCUSSION OF RESULTS

In the described experiments on tungsten subjected to a normal magnetic field, an electromagnetic wave excited acoustic vibrations of two types: a normal acoustic mode U_{1s} , propagating at the velocity of sound s_0 , and an anomalous mode U_{3s} , traveling at a phase velocity equal to the Fermi velocity of the conduction electrons $v \gg s_0$. The interaction between these two acoustic signals led to effects of the following three types: 1) an inversion of the $U(H)$ lines as a result of a change in the frequency by an amount of Δf and periodic recovery of the line profile with a period $2\Delta f$; 2) oscillations of the output acoustic signal $U(H)$ and of $\partial U(H)/\partial H$ in a magnetic field H , both characterized by a constant period; 3) a resonant change in the structure of the oscillations of $U(H)$ and $\partial U(H)/\partial H$ in a magnetic field H near $\omega \approx \Omega$.

1) Our experiments were carried out in the absence of a reference signal so that the observed dependences represented interference between the acoustic excitations U_{1s} of Eq. (9) and U_{3s} of Eq. (21). As shown in Sec. 2, $U_{1s}(H, \omega)$ obtained in a range of magnetic fields $H < 1$ kOe was a monotonic function of H and was linearly polarized, whereas the component U_{3s} oscillated as a function of H . Therefore, $U_{1s}(H)$ acted as the "reference signal" of frequency ω . An amplitude detector recorded a signal of the following form:

in the case of circular polarization of U_{3s}

$$U_s(H, \omega) = |U_{1s} + U_{3s}| \approx |U_{1s}| + |U_{3s}| \cos\left(\frac{\omega + s\Omega}{v} d - \frac{\omega d}{s_0}\right), \quad (25)$$

whereas in the linear polarization case, of U_{3s}

$$\begin{aligned} U_s(H, \omega) &= \frac{1}{2} |(U_{1s} + U_{3s})| \\ &\approx |U_{1s}| + |U_{3s}| \cos\left(\frac{\omega d}{v} - \frac{\omega d}{s_0}\right) \cos \frac{\Omega d}{v}. \quad (26) \end{aligned}$$

For simplicity, we assumed that $|U_{1s}| > |U_{3s}|$ in Eqs. (25) and (26).

A change in the frequency in Eq. (25) modulated the phase of the oscillations as a function of the magnetic field H , whereas in Eq. (26) there was modulation of the signal amplitude. It is clear from Eqs. (25) and (26) that a change in the frequency by an amount $\Delta\omega \approx \pi s_0/d$ should result in inversion of the oscillations. The validity of separation of the sound signal generated by electromagnetic excitation into the reference U_{1s} and oscillatory U_{3s} components was confirmed by the observation that the measured frequency of the line inversion $\Delta f \approx s_0/d$ yielded the velocity $s_0 \approx 2.88 \times 10^5$ cm/s, which was identical with the known value of the density of sound s_0 in tungsten along the [100] axis.¹²

2) Oscillations of the sound component U_{3s} in a field H appeared for the same reason as the harmonic distribution of the electromagnetic field in a metal.¹⁸ The distribution was due to the fact that the interaction of electrons was strongest for that harmonic of a wave packet for which the wavelength was equal to the extremal displacement of an electron outside the cyclotron period $2\pi\nu/\Omega$. The oscillations had a constant period in terms of the field H and this period was

$$\Delta H = \frac{\hbar}{ed} \frac{\partial S}{\partial k_z} = \frac{2\pi c\nu m}{ed}, \quad p = \hbar k, \quad (27)$$

where S is the area of a section of the Fermi surface $\varepsilon(\mathbf{k}) = \varepsilon_F$ out by the $p_z = \text{const}$ plane.

A spectral analysis made it possible to identify five oscillation periods corresponding to different sections of the Fermi surface of tungsten (sections A and B of the hole octahedron and an extremal section H of the electron "jack") and limiting points on the "bowl" of the electron "jack" (point G) and on the hole ellipsoids (point K). The quantities $(2\pi)^{-1} \partial S / \partial k_z = \xi$ found from the Fourier spectra were as follows: $\xi \approx 0.52 \text{ \AA}^{-1}$ for the section A ; $\xi \approx 0.168 \text{ \AA}^{-1}$ for the section B ; $\xi \approx 0.148 \text{ \AA}^{-1}$ for the section H ; $\xi \approx 0.186 \text{ \AA}^{-1}$ for the limiting point K ; $\xi \approx 1.10 \text{ \AA}^{-1}$ for the limiting point G . In the section A there were two harmonics A_1 and A_3 . For comparison, we shall now give the values of ξ obtained from the experiments on magnetoacoustic and size effects: $\xi = 0.475\text{--}0.512 \text{ \AA}^{-1}$ for the section A (Ref. 27); $\xi = 0.168 \pm 0.002 \text{ \AA}^{-1}$ in the section B (Ref. 28); $\xi = 0.143 \pm 0.002 \text{ \AA}^{-1}$ in the section H (Refs. 28 and 29); $\xi = 1.08 \text{ \AA}^{-1}$ for the limiting point G (Refs. 28 and 29). The calculated value $\xi = 1.192 \text{ \AA}^{-1}$ applies to the limiting points K (Ref. 30).

3) The resonant change in the oscillation amplitude U_{\parallel} (H) and in the derivative $\partial U_{\parallel} / \partial H$ in a field H near $\omega \approx \Omega$ was attributed to a diamagnetic resonance. Figure 1a shows the dependence of the derivative $\partial U_{\parallel} / \partial H$ on the magnetic field H at two frequencies. The characteristics of these curves were accounted for by an analysis of all the main diamagnetic resonance line profiles (Fig. 2). It was found that the experimental data in Fig. 1a were best described by a theoretical dependence $\partial U_{\parallel}(H) / \partial H$ when electromagnetic excitation of sound was due to electrons characterized by extremal drift (Fig. 2c) and a diamagnetic resonance was stronger than in the case of electrons from the vicinity of the limiting points and sections (Figs. 2a and 2b). Figure 1b gives the results of a theoretical calculation of the dependence of $\partial U_{\parallel} / \partial H$ on H . It is clear from this figure that the amplitude of $\partial U_{\parallel} / \partial H$ at $\omega = \Omega$ had a resonant peak of the envelope and the oscillation period near the resonance exhibited dispersion. The dispersion of the period was due to dispersion of the phase of the function $\Psi_{-}(H)$ of Eq. (21) (Fig. 2c).

A comparison of Figs. 1a and 1b demonstrated a good agreement between the theory and experiment. We therefore concluded that the observed singularity of $\partial U_{\parallel}(H) / \partial H$ (Fig. 1a) was governed by a diamagnetic resonance in the case of electromagnetic excitation of sound and was due to the transfer of acoustic excitation of carriers characterized by extremal drift. The value of the field $H \approx 160 \text{ Oe}$ corresponding to a diamagnetic resonance ($\omega = \Omega$) gave the cyclotron mass $m \approx 0.85m_0$ (m_0 is the mass of a free electron).

This value was close to $m \approx 0.93m_0$ representing the cyclotron mass of holes following ν orbits on the octahedron, as determined in the experiments on the de Haas–van Alphen effect.³⁰ Clearly, this resonance and the oscillations were due to the B orbits of the hole octahedron, which were localized on the Fermi surface close to the ν orbits. Since the momentum p_z was governed by the oscillation period of Eq. (27), we could estimate the drift velocity for this group of holes: $v \approx 0.2 \times 10^8 \text{ cm/s}$. This velocity was less than the velocity of carriers in the vicinity of limiting points of the hole octahedron amounting to $v \approx 1.0 \times 10^8 \text{ cm/s}$ (Ref. 31).

The penetrating component of the electromagnetic field $E(z)$ was known to exist in the absence of a magnetic field³² and also for orientations of the field \mathbf{H} relative to the surface of the metal other than those investigated by us. It therefore follows that in such cases we could expect generation of anomalous (fast) sound in a metal.

The authors are grateful to V. F. Gantmakher for discussing the paper and for valuable advice.

- ¹V. M. Kontorovich and N. A. Tishchenko, *Izv. Vyssh. Uchebn. Zaved. Radiofiz.* **6**, 24 (1963).
²V. G. Skobov and É. A. Kaner, *Zh. Eksp. Teor. Fiz.* **46**, 273 (1964) [*Sov. Phys. JETP* **19**, 189 (1964)].
³A. N. Vasil'ev and Yu. P. Gaïdukov, *Usp. Fiz. Nauk* **141**, 431 (1983); **150**, 161 (1986) [*Sov. Phys. Usp.* **26**, 952 (1983); **29**, 889 (1986)].
⁴V. F. Gantmakher and V. T. Dolgoplov, *Pis'ma Zh. Eksp. Teor. Fiz.* **5**, 17 (1967) [*JETP Lett.* **5**, 12 (1967)].
⁵V. F. Gantmakher and V. T. Dolgoplov, *Zh. Eksp. Teor. Fiz.* **57**, 132 (1969) [*Sov. Phys. JETP* **30**, 78 (1970)].
⁶G. I. Babkin, V. T. Dolgoplov, and V. Ya. Kravchenko, *Pis'ma Zh. Eksp. Teor. Fiz.* **13**, 563 (1971) [*JETP Lett.* **13**, 402 (1971)].
⁷M. I. Kaganov, V. B. Fiks, and N. I. Shikina, *Fiz. Met. Metalloved.* **26**, 11 (1968).
⁸É. A. Kaner and V. L. Fal'ko, *Zh. Eksp. Teor. Fiz.* **64**, 1016 (1973) [*Sov. Phys. JETP* **37**, 516 (1973)].
⁹V. L. Fal'ko and V. A. Yampol'skiĭ, *Fiz. Nizk. Temp.* **3**, 477 (1977) [*Sov. J. Low Temp. Phys.* **3**, 231 (1977)].
¹⁰N. C. Banik and A. W. Overhauser, *Phys. Rev. B* **18**, 3838 (1978).
¹¹V. L. Fal'ko, *Zh. Eksp. Teor. Fiz.* **85**, 300 (1983) [*Sov. Phys. JETP* **58**, 175 (1983)].
¹²A. V. Golik, A. P. Korolyuk, V. L. Fal'ko, and V. I. Khizhnyiĭ, *Zh. Eksp. Teor. Fiz.* **86**, 616 (1984) [*Sov. Phys. JETP* **59**, 359 (1984)].
¹³É. A. Kaner, V. L. Fal'ko, and L. P. Saĭnikova, *Fiz. Nizk. Temp.* **12**, 831 (1986) [*Sov. J. Low Temp. Phys.* **12**, 471 (1986)].
¹⁴D. Kubinski and J. Trivisonno, *Phys. Rev. B* **35**, 9014 (1987).
¹⁵V. D. Fil', N. G. Burma, and P. A. Bezuglyĭ, *Pis'ma Zh. Eksp. Teor. Fiz.* **23**, 428 (1976) [*JETP Lett.* **23**, 387 (1976)].
¹⁶É. N. Bogachek, A. S. Rozhavskii, and R. I. Shekhter, *Pis'ma Zh. Eksp. Teor. Fiz.* **23**, 432 (1976) [*JETP Lett.* **23**, 391 (1976)].
¹⁷T. M. Irklienko, A. P. Korolyuk, and V. I. Khizhnyiĭ, *Pis'ma Zh. Eksp. Teor. Fiz.* **46**, 114 (1987) [*JETP Lett.* **46**, 140 (1987)].
¹⁸É. A. Kaner and V. F. Gantmakher, *Usp. Fiz. Nauk* **94**, 193 (1968) [*Sov. Phys. Usp.* **11**, 81 (1968)].
¹⁹T. G. Phillips, G. A. Baraff, and P. H. Schmidt, *Phys. Rev. B* **5**, 1283 (1972).
²⁰I. E. Aronov, A. V. Golik, A. P. Korolyuk, and V. L. Fal'ko, *Fiz. Nizk. Temp.* **14**, 313 (1988) [*Sov. J. Low Temp. Phys.* **14**, 173 (1988)].
²¹A. V. Golik, A. P. Korolyuk, and V. I. Khizhnyiĭ, *Prib. Tekh. Eksp. No.* **2**, 213 (1987).
²²É. A. Kaner, *Zh. Eksp. Teor. Fiz.* **43**, 216 (1962) [*Sov. Phys. JETP* **16**, 154 (1963)].
²³L. T. Tsybal and T. F. Butenko, *Solid State Commun.* **13**, 633 (1973).
²⁴G. L. Kotkin, *Zh. Eksp. Teor. Fiz.* **41**, 281 (1961) [*Sov. Phys. JETP* **14**, 201 (1962)].
²⁵A. A. Abrikosov, *Fundamentals of the Theory of Metals* [in Russian], Nauka, Moscow (1987).
²⁶T. Kjeldaa Jr., *Phys. Rev.* **113**, 1473 (1959).
²⁷S. W. Hui and J. A. Rayne, *J. Phys. Chem. Solids* **33**, 611 (1972).

²⁸T. F. Butenko, V. T. Vitchinkin, A. A. Galkin, *et al.*, Zh. Eksp. Teor. Fiz. **78**, 1811 (1980) [Sov. Phys. JETP **51**, 909 (1980)].

²⁹I. M. Vitebskiĭ, V. T. Vitchinkin, A. A. Galkin, *et al.*, Fiz. Nizk. Temp. **1**, 400 (1975) [Sov. J. Low Temp. Phys. **1**, 200 (1975)].

³⁰R. F. Girvan, A. V. Gold, and R. A. Phillips, J. Phys. Chem. Solids **29**, 1485 (1968).

³¹V. V. Boĭko and V. A. Gasparov, Zh. Eksp. Teor. Fiz. **61**, 2362 (1971) [Sov. Phys. JETP **34**, 1266 (1972)].

³²G. E. M. Reuter and E. H. Sondheimer, Proc. R. Soc. London Ser. A **195**, 336 (1948).

Translated by A. Tybulewicz